Biochimica et Biophysica Acta, 973 (1989) 93–104
Elsevier

BBA 42891

Picosecond dynamics of directed excitation transfer in spectrally heterogeneous light-harvesting antenna of purple bacteria

A. Freiberg [1], V.I. Godik [2], T. Pullerits [1] and K. Timpman [1]

[1] *Institute of Physics, Estonian SSR Academy of Sciences, Tartu, and* [2] *A.N. Belozersky Laboratory of Molecular Biology and Bioorganic Chemistry, Moscow State University, Moscow (U.S.S.R.)*

(Received 15 August 1988)

Key words: Photosynthesis, bacterial; Excitation transfer; Picosecond fluorescence; Fluorescence; Light harvesting antenna; Excitation annihilation; (*Rb. sphaeroides*); (*Chr. minutissimum*)

Picosecond spectrally resolved fluorescence kinetics measurements, together with model simulations of the obtained data, based on coupled rate equations, have been employed to determine the rates and the pathways of heterogeneous excitation transfer in *Rhodobacter sphaeroides* and *Chromatium minutissimum*. The presence of a directed excitation flow from the short-wavelength bacteriochlorophyll forms to the long-wavelength one and from the latter to reaction centres has been revealed. As a result, the overall excitation trapping time in the bacteria investigated has been found to be about 60 ps both at 77 K and at room temperature, i.e. the same as in *Rhodospirillum rubrum*, although the number of antenna bacteriochlorophyll molecules per reaction centre is several times larger. A comparison of the experimental and theoretical kinetic data shows that, besides obvious spectral heterogeneity of the bacteriochlorophyll antenna represented by well-resolved B800, B850 and B875 spectra forms, an intrinsic spectral inhomogeneity of these forms is likely to play an essential role in the excitation transfer. The obtained picture of the mutual arrangement of different complexes in membranes is similar to the one suggested earlier, except that the presence of at least two types of B800-850 complexes, the ones closely associated with B875 and the more remote ones, has been discovered. The excitation transfer to B875 has been shown to take about 10 and 50 ps for the first and the second type of B850 molecules, respectively. The intracomplex B800 → B850 transfer time is an order of magnitude smaller, about 1 ps. These three time constants seem to be practically independent of the reaction centre state and the temperature in the 300 K–77 K interval. At high excitation intensities (more than $1 \cdot 10^{10}$ photons per pulse) a shortening of the long-wavelength fluorescence decay time and a short-wavelength shift of the corresponding band maximum have been observed. Both effects are due to the annihilation of singlet and triplet excitations.

Introduction

The main principles of the very efficient conversion of light energy into an electrochemical form by photosynthetic organisms continue to be the subject of intense investigations. One of these principles is the separation in space of two main structural parts of the primary photosynthetic apparatus, whose major functions are: (i) to absorb the solar light, and (ii) to convert the absorbed energy into the potential energy of spatially separated electrical charges. Most of the light quanta are known to be absorbed by the pigment molecules of the so-called light-harvesting or antenna pigment-protein complexes, while conversion of the absorbed energy is performed by special pigment-protein complexes of the so-called reaction centres (RCs).

The advantages of such separation, considered in detail earlier [1], are evident, but a new problem inevitably arises: how to transport the light energy absorbed by antenna pigments to RC pigments with minimal losses. The high yield (more than 90%) of the primary charge separation in RCs could be attained only if the rate of excitation trapping by open RCs is at least an order of magnitude higher than that of other losses in the antenna. Much theoretical and experimental evidence has been obtained (for the latest review, see Ref. 2), which suggests that the underlying mechanism is the resonance excitation transfer via chlorophyll singlet states. For the case of purple bacteria this point has recently been quantitatively settled [3,4].

Correspondence: A. Freiberg, Institute of Physics, Estonian SSR Academy of Sciences, 202400 Tartu, U.S.S.R.

In the case of a homogeneous antenna the rate of excitation trapping is directly proportional to the number of light-harvesting molecules per RC (see, e.g., Ref. 2). This fact seems to explain why all the known large (larger than 20–40 pigment molecules per RC) photosynthetic light-harvesting antennae are explicitly spectrally heterogeneous. The role played by the spectral heterogeneity of the light-harvesting antenna in the shortening of the time interval, necessary for excitation trapping, has been studied theoretically in Refs. 5–7.

It is reasonable to begin the experimental elucidation of the problem with the most simply organized and carefully studied purple bacteria. The antenna of bacteriochlorophyll (BChl) *a*-containing purple photosynthetic bacteria consists of two main pigment-protein complexes, B800-850 and B875 (characterized by absorption maxima in the near-infrared range at about 800 nm, 850–860 nm and 870–890 nm, respectively). Some strains, such as *Rhodospirillum rubrum*, contain a single antenna complex of the B875 type, which usually occurs in a fixed stoichiometry of 20–30 BChl molecules per RC complex [8]. The size of photosynthetic units for these bacteria is known to be practically independent of growth conditions, contrary to purple bacteria containing both the B800-850 and B875 light-harvesting complexes. In the latter case, the size of the photosynthetic unit can be varied in a wide range at the expense of B800-850 complexes by changing the incident photon flux and oxygen partial pressure. Both the B875 and the B800-850 complexes contain two pigment-binding polypeptides, α- and β-subunits, with a molecular mass of 6–12 kDa. Each pair of the polypeptides binds two (B875) or three (B800-850; one B800 and two B850) BChl molecules and, respectively, one or two molecules of carotenoids [8]. Although the composition and the structure of the light-harvesting antennae of purple bacteria have been actively studied, there is still only poor evidence regarding the mutual arrangement of different pigment-protein complexes in membranes and excitation energy transfer pathways between them.

On the basis of stationary fluorescence data it has been concluded that RCs are surrounded and interconnected by B875 complexes, B800-850 complexes being arranged peripherally and interconnecting several RC-B875 complexes [9,10]. Recent investigations with the use of the mutant strains of *Rhodobacter sphaeroides* [11] and *Rb. capsulata* [12] are in agreement with these suggestions. As to the kinetics of the excitation transfer from B800-850 to B875 and from the latter to RCs, the available experimental evidence is scanty and inconsistent. Thus, Zankel and Clayton [10] have concluded that these processes are rather slow: the 'average' time constant is taken to be equal to about 1 ns. The rate constant of B850 → B875 excitation transfer in *Rb. sphaeroides* has been assumed to be approximately equal to that of excitation trapping by open RCs. Contrary to this, Monger and Parson [9] have suggested from their singlet-triplet annihilation studies that the lifetime of excitations in B800-850 is much shorter than in B875. In accordance with this suggestion it has been shown [4] that the kinetics of picosecond fluorescence under uniform excitation and broad-band spectral recording is similar in both *Rb. sphaeroides* and *R. rubrum*, in spite of the large difference in the size of the photosynthetic unit. A conclusion that excitations are transferred from B850 to B875 in several picoseconds has been drawn by Sebban and Moya [13].

The first direct measurements of the B850 → B875 transfer kinetics, performed with the use of spectrally-resolved picosecond fluorescence [14,15] and picosecond absorption [16,17] techniques, have also produced contradictory results in a number of important aspects. Firstly, in qualitative agreement with Zankel and Clayton [10], in Ref. 16 the B850 → B875 transfer time has been determined to be nearly as large as the macroscopic time of excitation trapping by open RCs (which had earlier been shown to be equal to 60 ps [3,4]). According to picosecond fluorescence studies [14,15], this time is several times shorter and does not exceed 10 ps for most excitations. Secondly, it was claimed by Sundstrom et al. [16] that even with open traps the equilibration process of excitations at room temperature between B800-850 and B875 produces the biphasic B875 excited state decay and an apparent increase in the time constant describing the trapping process up to approx. 120 ps. In our experiments such increases have not been observed.

In order to clarify these contradictory data, in the present work a more thorough analysis of picosecond dynamics in excitations in the heterogeneous light-harvesting antenna of purple bacteria *Rb. sphaeroides* and *Chromatium minutissimum* * has been carried out, including a theoretical simulation of the investigated processes, based on the coupled kinetic rate equation model. This approach allows one to construct a consistent picture of the directed excitation energy transfer in these bacteria both at room temperature and at 77 K.

Materials and Methods

Purple bacteria *Rb. sphaeroides* and *Chr. minutissimum* (wild types, Moscow University collection) were

* *Chr. minutissimum* has an advantage over *Rb. sphaeroides* in that it has more separated and clear-cut absorption spectral bands. Recently it has been suggested that *Chr. minutissimum*, unlike other known purple photosynthetic bacteria, has two different types of RCs (see, e.g., Ref. 45). This has not been confirmed in our measurements. Quite similar data have been obtained on both *Rb. sphaeroides* and *Chr. minutissimum*.

cultivated and chromatophores isolated as described in Ref. 4. Concentrated chromatophore suspensions were diluted before measurements by Tris-HCl buffer, pH 7.5, or by a mixture of the buffer and glycerol, 1 : 3 v/v, for low-temperature measurements. Most of the room temperature experiments were made with the use of a flow-cell in order to exclude the possible effects of high excitation intensity [4].

Picosecond fluorescence kinetics were measured by a picosecond spectrochronograph described in detail in Ref. 18. The picosecond pulse source was a mode-locked continuous-wave oxazine 750 dye laser (pulse duration 3 ps), synchronously pumped by a krypton-ion laser at 82 MHz. The emission, viewed at an angle of 90° with respect to the exciting beam in a reflection mode, was filtered by two single-grating monochromators. In order to remove the excess pulse broadening in the monochromators, they were combined in a subtractive dispersion mode. Fluorescence was recorded in the 780–1000 nm range by a unit consisting of a synchroscan streak camera, a SIT vidicon, and a minicomputer-supported optical multichannel analyzer. In every case several decay curves were recorded and intercompared to avoid accidental results. The typical exciting light intensity was in the range of $5 \cdot 10^8$–10^{10} photons per cm^2 per pulse, which excludes non-linear processes but, due to the 82 MHz pulse repetition rate, provides the conditions of saturated (RCs photooxidized) photosynthesis, unless approx. 10^{-3} M of $Na_2S_2O_4$ is added to the suspensions. Under the latter conditions the excitation quenching was shown to proceed very much as in the case of active photosynthesis with open RCs, the quenching time being only about 20% longer [4], presumably due to the reduction in the rate of charge separation induced by the electrostatic repulsion of negative charge on the primary quinone acceptor. An essential sample-to-sample variability of the fluorescence decay times was observed: when RCs were closed, the variability of the B875 fluorescence decay time was in the range of 150–250 ps. It was also found to depend on the preexcitation conditions during freezing up to 77 K.

The decay profiles were computer-simulated by a sum of exponentials $I(t) = \Sigma_i A_i \exp(-t/\tau_i)$, taking into account the convolution with apparatus response function of about 15 ps full width at half intensity maximum. The terms A_i correspond to the initial amplitudes of the individual components, the decays of which are characterized by the lifetimes τ_i. The uncertainty of the parameters derived from the analysis of the measured multi-exponential kinetics was about 30% for the decay times of about 10 ps, around 20% for those of several tens of picoseconds, and better than 10% for the decay times of about 200 ps and longer. The accuracy of the determination of the corresponding amplitude ratios was about 30%.

Results and Discussion

Fluorescence kinetics at low temperatures

As has already been shown [14,15], the fluorescence kinetics of the purple bacteria containing three distinct antenna BChl spectral forms depends on the recording wavelength in a complex fashion even at low temperatures when the energetically uphill excitation transfer is practically eliminated. Fig. 1A shows the results obtained with *Chr. minutissimum* chromatophores, excited by 772 nm light at 77 K (excitation at 796 nm, which selectively excites B800 BChl molecules, gave similar results). Four wavelengths, at which the fluorescence decay kinetics have been observed, are marked by arrows at the stationary fluorescence spectrum, presented in Fig. 1C. The decay is well approximated by a single exponential component with the time constant of 190 ps at wavelengths longer than 930 nm, the latter corresponding to the wavelength of the maximum in the fluorescence spectrum at 77 K. In this spectral range, a fluorescence rise with the time constant of about 10 ps is also observed. The time constant of the fluorescence decay in the long-wavelength part of the spectrum is in close agreement with the values previously determined

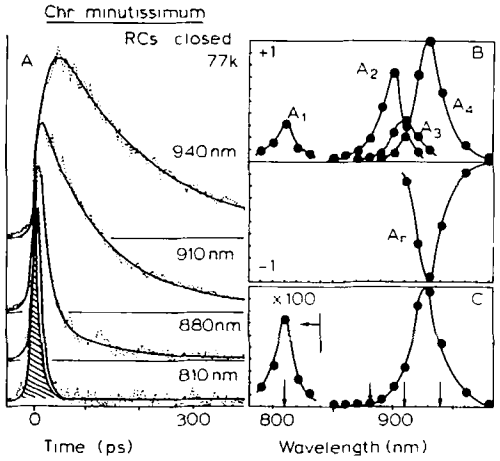

Fig. 1. (A) Experimental fluorescence kinetics (dotted curves) of *Chr. minutissimum* chromatophores at 810, 880, 910 and 940 nm, recorded with 8 nm spectral resolution. RCs are closed, temperature is 77 K. Continuous curves represent the result of computer-simulation of the experiment by a sum of exponentials (see Materials and Methods): at 810 nm, a single-exponential decay with $\tau_1 = 5$ ps; at 880 nm, a three-exponential decay with $\tau_2 = 9$ ps; $\tau_3 = 65$ ps, $\tau_4 = 190$ ps and the amplitude ratio $A_2/A_3/A_4 = 85:14:1$; at 910 nm, a three-exponential decay with $\tau_2 = 6$ ps, $\tau_3 = 65$ ps, $\tau_4 = 200$ ps and $A_2/A_3/A_4 = 35:40:25$; at 940 nm, an exponential rise with $\tau_r = 10$ ps and decay with $\tau_4 = 190$ ps. An excitation of 772 nm and of 0.4 W/cm^2 intensity was used. The apparatus response is also shown (shaded). (B) Spectral distribution of the relative amplitudes of separate fluorescence components, characterized by different computer-simulated fluorescence decay (A_1–A_4) and rise (A_r) times. The lifetime-dependent amplitude suppression has been corrected taking into account the real apparatus response function, as shown in part A. (C) the time-integrated fluorescence spectrum (see the text). Arrows indicate the wavelengths for which the kinetic curves are shown in part A.

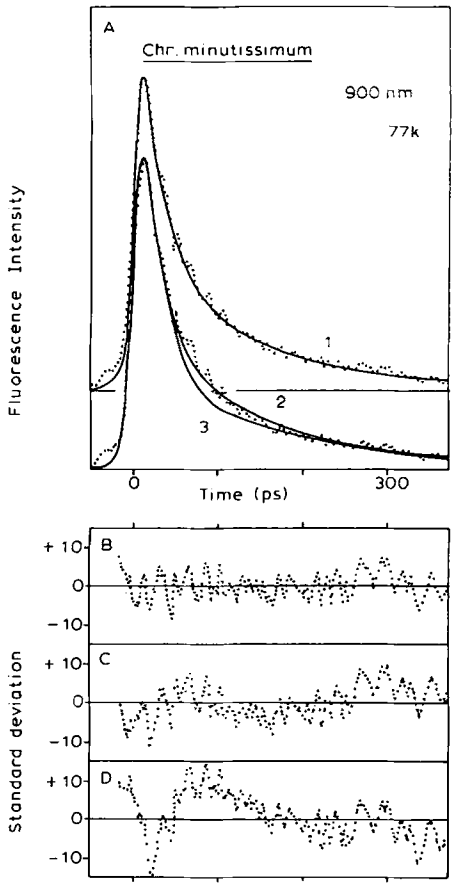

Fig. 2. Experimental fluorescence kinetics (dotted curves) for *Chr. minutissimum* chromatophores with closed RCs at 77 K, measured at 900 nm, in comparison with different computer-simulated approximation curves: 1, a three-exponential fit with $\tau_1 = 6$ ps, $\tau_2 = 50$ ps, $\tau_3 = 190$ ps and $A_1/A_2/A_3 = 70:23:7$; 2, a two-exponential fit with $\tau_1 = 20$ ps, $\tau_2 = 120$ and $A_1/A_2 = 72:28$; 3, a two-exponential fit with $\tau_1 = 25$ ps, $\tau_2 = 180$ ps and $A_1/A_2 = 85:15$. Parts B, C and D demonstrate the approximation precision respectively for curves 1, 2 and 3.

for excitation quenching by closed photooxidized RCs at room temperature in *R. rubrum* and *Rb. sphaeroides* [3,4].

At wavelengths shorter than 930 nm the kinetics is more complex. In particular, at 910 nm a triple-exponential decay with some rise is necessary to fit the data, the corresponding decay constants being 6 ps, 65 ps, and 200 ps (Fig. 1A). As demonstrated in Fig. 2, the double-exponential decay fitting satisfies the experimental data at 900 nm only if instead of the 190 ps decay component the presence of a much more short-lived 120 ps component is assumed. Since the 190 ps component should make some contribution at 900 nm (see Fig. 1B), the latter assumption is not justified. At 865–890 nm the fluorescence kinetics can satisfactorily be described by two exponentials with the decay constants 5–9 ps and 50–70 ps (Fig. 1A, B), the single-exponential approach being inadequate. Only around 800 nm is the decay single-exponential with a time constant of about 5 ps (Fig. 1A).

The spectral dependence of the deconvoluted amplitudes for all the above-mentioned (averaged) decay components is shown in Fig. 1B. It can be seen that the most-short-lived (about 5 ps) component belongs to B800 and the most long-lived (about 190 ps) one, to B875. Two components, those of about 8 ps and 60 ps lifetimes, are due to the B850 decay. It appears that there exist two spectrally alike pools of the B800-850 complexes, which are characterized by different rates of excitation transfer from B850 to B875: nearly 70% of the B850 excitations are transferred to B875 in about 8 ps, while the rest, about 30% of excitations, are transferred in about 60 ps.

The time-integrated fluorescence spectrum constructed from the computer-analyzed experimental data (see Materials and Methods) as

$$I(\lambda) = \int_0^\infty I(\lambda, t)\,dt = \sum_i A_i \int_0^\infty \exp(-t/\tau_i)\,dt = \sum_i A_i \tau_i$$

is similar to the one measured with the conventional spectrometer (Fig. 1C). However, according to the model calculations described below, the amplitude A_1 in Fig. 1B should be even higher than the amplitude A_4. From this comparison one can conclude that the deconvoluted decay time, 5 ps, of the B800 fluorescence is resolution-limited and, therefore, 3–4-times overestimated. If this is taken into account, one obtains a B800 fluorescence decay time of 1–2 ps. This number correlates well with the estimation of B800 → B850 energy transfer time, made in Ref. 19.

Quite similar data have been obtained with *Rb. sphaeroides*. The results of the deconvolution of the measured fluorescence kinetics into exponential terms

TABLE I

Summary of the approximation parameters (1/e lifetimes and relative amplitudes) of the experimental fluorescence kinetics of Chr. minutissimum chromatophores with closed RCs at 77 K

λ (nm)	τ_1 (ps)	τ_2 (ps)	τ_3 (ps)	τ_4 (ps)	A_1	A_2	A_3	A_4
800	6				100			
810	4				100			
820	6				100			
830	5				100			
850		10				100		
860		11				100		
870		8	70	190		90	9	1
880		9	65	190		85	14	1
890		5	50	190		84	13	3
900		7	55	200		70	23	7
910		6	65	200		35	40	25
920		9	60	180		−79	21	79
930		9	60	190		−93	7	93
940		10		190		−100		100
960		11		190		−100		100
980		7		180		−100		100

for both of *Chr minutissimum* and of *Rb. sphaeroides* at 77 K are given respectively in Tables I and II. The region around 800 nm is poorly analyzable in the case of *Rb. sphaeroides* because of the interference of the B800 fluorescence with the parasitic one from a BChl product, which has an absorption maximum at about 780 nm.

Model simulation of the low temperature kinetics

An analysis of fluorescence decay curves as a function of the recording wavelength at 77 K has made it possible to derive a set of important parameters necessary to develop a kinetic model for describing the underlying excitation transport and quenching processes. The simplest kinetic scheme which may be suggested is of the following form:

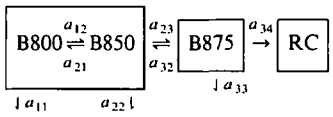

(1)

Here B800, B850, and B875 are distinct BChl pigment pools within B800-850 and B875 pigment-protein complexes (indicated by frames); a_{ij} are the macroscopic time-independent rate constants of the excitation transfer from pool i to pool j (except a_{34}, which designates the average rate constant of excitation quenching by open or closed RCs); a_{ii} are the rate constants of trivial losses, such as fluorescence and intramolecular energy conversion, which were taken to be $(0.85\ \text{ns})^{-1}$ at 77 K [20] for all antenna molecules.

The way of solving the corresponding system of three coupled kinetic rate equations and of comparing the theoretical results with the experimental data are given in the Appendix. This comparison persuades us that, based on scheme (1), it is not possible to describe the peculiarities of the experimental kinetic data, especially

TABLE II

Summary of the approximation parameters (1/e lifetimes and relative amplitudes) of the experimental fluorescence kinetics of Rb. sphaeroides chromatophores with closed RCs at 77 K

λ (nm)	τ_1 (ps)	τ_2 (ps)	τ_3 (ps)	τ_4 (ps)	A_1	A_2	A_3	A_4
790	8			180	73			27
850		12	45			93	7	
860		8	60	220		89	9	2
870		12	40	220		80	18	2
880		10	45	200		76	19	5
890		5	40	200		50	34	16
900		9	55	220		12	29	59
910		13	70	210		−84	16	84
920		13		210		−100		100
940		10		220		−100		100
960		9		210		−100		100

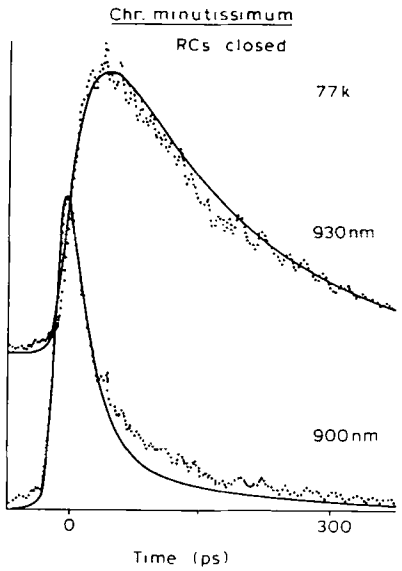

Fig. 3. Experimental fluorescence kinetics (dotted curves) of *Chr. minutissimum* chromatophores in comparison with calculated (according to model kinetic scheme (1)) approximation curves (continuous line) at 900 and 930 nm. Other experimental conditions as in Fig. 1. Best attainable fit time constants: $1/a_{12} = 1$ ps, $1/a_{23} = 25$ ps, $1/a_{34} = 170$ ps. The relative number of BChl molecules in pools B800, B850 and B875 is 1 : 2 : 1.

at wavelengths longer than 860 nm. This can be clearly seen in Fig. 3, where the experimental decay curves for *Chr. minutissimum* are approximated by the theoretical ones according to scheme (1).

A more satisfactory fit between the experimental and the model decay curves could be achieved if, instead of a single type of B800-850 pigment-proteins, the existence of at least two types of B800-850 pigment-proteins with different kinetic (and spectral) characteristics is assumed. This suggestion ensues from our experimental findings (see Fig. 1 and Refs. 14 and 15) and is in agreement with structural data in Refs. 21 and 22. According to this, the single-channel scheme (1) has been changed to a two-channel (A and B) one as follows:

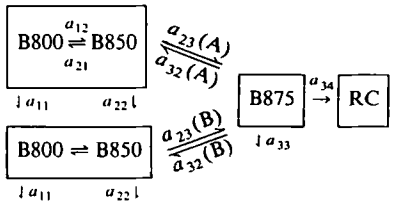

(2)

The parameters of this model are: (i) the excitation transfer and quenching rate constants a_{12}, $a_{23}(A)$, $a_{23}(B)$, a_{34}; (ii) the ratio of the B800-850 complexes in the channels A and B; and (iii) the position of the peak of the absorption spectrum of B850 pigment molecules in channel B as compared with this maximum in channel A. The spectral characteristics of B800, considered

to be the same in both channels, B850(A) and B875 pigments as well as the rate constants $a_{11} = a_{22} = a_{33}$ have been drawn from experiments as quoted in the Appendix. The fluorescence band red-shift and the absorption and fluorescence band widths were taken to be equal for all the B850 pigments. The relative number of B800, B850 and B875 pigment molecules in the photosynthetic unit was estimated to be equal to 1 : 2 : 1, according to the experimental optical absorption spectra of our samples.

With the use of scheme (2) a good agreement of model calculations with experiments can be attained. In Fig. 4, such a comparison for *Chr. minutissimum* at four selected fluorescence recording wavelengths is depicted. The theoretical curves * suggest that the time constant of B800-850 → B875 transfer in channels A and B are 10 and 45 ps, respectively, and that the ratio of the B800-850 complexes is (3–4) : 1 in favour of channel A. Moreover, for a good agreement it is obligatory to shift the absorption (and fluorescence) maxima of the channel B B850 molecules by some 5–7 nm towards longer wavelengths in comparison with B850 molecules in channel A. Otherwise no satisfactory good fit with the experimental data can be achieved. Besides the kinetic curves, Fig. 4 shows also the stationary fluorescence spectrum obtained with the use of relation (A5) (Fig. 4C), as well as the amplitude spectra of all the decay components which are the solutions of the system of the coupled rate equations (A2) describing the model scheme (2) (Fig. 4B). The negative amplitudes in Fig. 4B mean that the corresponding components manifest themselves in the kinetics as a fluorescence rise. Such amplitude spectra permit easy tracking of a complex interplay between different decay components with a change in the recording wavelength. The spectra presented in Fig. 4B are in good qualitative agreement with those in Fig. 1B, taking into account the limited (3–5 ps) time resolution of the experimental set-up and the basic difficulties

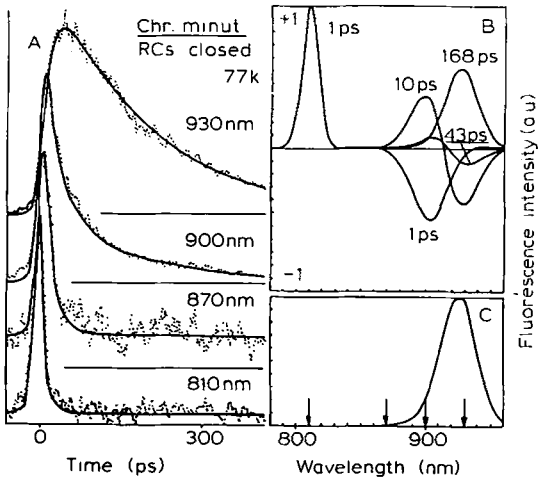

Fig. 4. (A) Experimental fluorescence kinetics (dotted curves) of *Chr. minutissimum* chromatophores at 77 K at the indicated recording wavelengths (other experimental conditions as in Fig. 1) together with the simulated model (according to kinetic scheme (2), see the text) approximation curves (continuous). The following best fit model parameters were used: $1/a_{12} = 1$ ps, $1/a_{23}(A) = 10$ ps, $1/a_{23}(B) = 45$ ps, $1/a_{34} = 210$ ps, $1/a_{ii} = 850$ ps, the relative number of BChl molecules in pools B800, B850 and B875, 1 : 2 : 1, the ratio of B800-850 (A) and B800-850 (B) complexes, 3 : 1. (B) The spectral distribution of the relative amplitudes of the different fluorescence components of the model curves, calculated with the use of the above-listed parameters. The numerical values above the curves denote the corresponding lifetimes. (C) The calculated time-integrated fluorescence spectrum.

with the analysis of multi-exponential fluorescence rise and decay curves [23].

The whole scope of the data presented suggests that kinetic Scheme 2 is the simplest one, sufficient to describe the main features of excitation dynamics in the heterogeneous light-harvesting antenna of *Chr. minutissimum* at 77 K. With the exception of some minor differences, the same is true for *Rb. sphaeroides* (cf. e.g., Tables I and II).

Fluorescence kinetics at room temperature

The presence of intense temperature-induced uphill excitation transfer at room temperature together with the broadening of pigment spectral bands makes the wavelength dependence of the fluorescence decay less distinct, which considerably complicates the constructive analysis of the experimental kinetics. At most wavelengths studied a triple-exponential decay and a complex fluorescence rise are expected. The parameters of the decomposition of *Rb. sphaeroides* fluorescence kinetics into three exponential components at room temperature, as described in Materials and Methods, are given in Table III. A shortening of τ_3 and τ_4 as compared to the 77 K data, as well as the change of the corresponding amplitude ratios is observed. Our experience shows [4] that the shortening of τ_4 is most probably due to the different samples employed at these measurements (cells vs. chromatophores) and it is not a temperature effect.

* In fact, for simplicity the theoretical curves in Figs. 4, 5, 7 and 8 were calculated not on the basis of scheme (2), but according to the following scheme (3) with two parallel antennae:

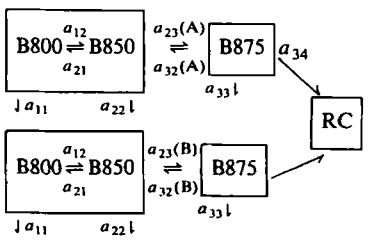

(3)

It can be shown that under the present conditions the difference between the theoretical results according to schemes (2) and (3) do not exceed the uncertainty of the experimental data.

TABLE III

Summary of the approximation parameters (1/e lifetimes and relative amplitudes) of the experimental fluorescence decay kinetics of Rb. sphaeroides cells with closed RCs at room temperature

λ (nm)	τ_1 (ps)	τ_2 (ps)	τ_3 (ps)	τ_4 (ps)	A_1	A_2	A_3	A_4
790	8			180	70			30
800	5			160	71			29
810	9			180	66			34
835		9	30	150		37	26	37
840		7	30	150		15	49	36
850		9	35	150		16	48	36
860		7	30	150		−43	57	43
870		9	35	150		−62	38	62
880		10	50	140		−91	9	91
890		14	50	150		−96	4	96
900		12		140		−100		100
910		12		150		−100		100
920		13		150		−100		100
930		13		150		−100		100
940		12		140		−100		100
960		14		150		−100		100

The kinetic model of scheme (2) with necessary modifications has also been applied to the description of the room temperature data. Fig. 5A shows that the experimental curves for *Rb. sphaeroides* are well approximated by the model ones. The same holds for *Chr. minutissimum*. In both samples, the same values of rate constants of the downhill energy transfer, a_{12} and a_{23}, as at 77 K were used. At the same time, the rate constants of the uphill transfer a_{ji} undergo changes with temperature due to the broadening and shift of the corresponding spectral bands. The amplitude spectra for separate decay components, calculated according to equation (A6), are presented in Fig. 5B. It can be seen that the most long-lived fluorescence component with 155 ps decay time is observed almost throughout the whole fluorescence spectrum. The calculated and measured fluorescence decay times of B850 are shorter than those at 77 K, which is the manifestation of the uphill excitation transfer. Table III and Fig. 5 are in reasonable qualitative agreement with each other at wavelengths longer than 840 nm.

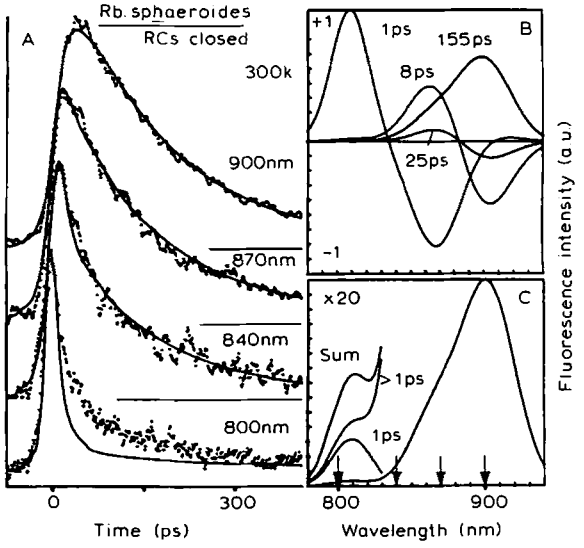

Fig. 5. (A) Experimental fluorescence kinetics (dotted curves) of *Rb. sphaeroides* cells with closed RCs at room temperature together with simulated model curves (continuous). Excitation conditions as in Fig. 1, recording resolution 4 nm, a flow-cell is used. Approximation kinetics parameters as in Fig. 4, except that the time constant of B875 excitation quenching $1/a_{34} = 135$ ps and $1/a_{ji} = 650$ ps [20]. (B) and (C) The same as in the preceding figure, except that the intensity of the time-integrated spectrum in the 800 nm region is 20-times magnified in order to demonstrate separately the contribution of direct B800 emission and of B800 emission due to back-transfer of excitations from B850 and B875 to the total intensity.

However, it seems that around 860–880 nm there is a quantitative controversy between the data of Fig. 5B and Table III. In the real experiment it is practically impossible to resolve the two or more decay components with close decay times and amplitudes [23]. Therefore in this case the quality of the model can be settled only the comparison of calculated and measured kinetics at a given wavelength as is done in Fig. 5A. One can see that the agreement is reasonably good. In fact, there may be a cause for an excessive shortening of the calculated decay times of B850 excited states in comparison with the measured decay times. This happens when the probability of the uphill energy transfer is overestimated. That this is indeed the case in our model will be shown below.

Fluorescence kinetics in the region around 800 nm needs special consideration. Unlike the situation at 77 K, due to an effective uphill energy transfer at 300 K, a simultaneous contribution of all other decay components to the B800 fluorescence decay is expected. Besides, as was already noted, in this region an emission of a nonphotosynthetic origin has been observed. The latter probably explains the observed discrepancy between the model and experimental kinetics at 800 nm (Fig. 5A). However, the calculated time-integrated fluorescence spectrum in Fig. 5C has an intensity twice as high as the experimental one at about 800 nm [10]. From Fig. 5C it follows that the longer-lived fluorescence components make up more than 50% of the total signal intensity at these wavelengths, which indicates that the role of the uphill energy transfer in our model may be overestimated. This complication can easily be surpassed if the possible intrinsic inhomogeneity of the spectral bands (above clear-cut B800, B850, B875 structure) is taken into account. This provokes localization of excitations in the longest-wavelength BChl forms within the B875 spectral band and diminishes the uphill energy transfer. This point will be further considered below.

The effect of the RC state

It was stated earlier that the wavelength dependence of the fluorescence kinetics of *Rb. sphaeroides* [14] and

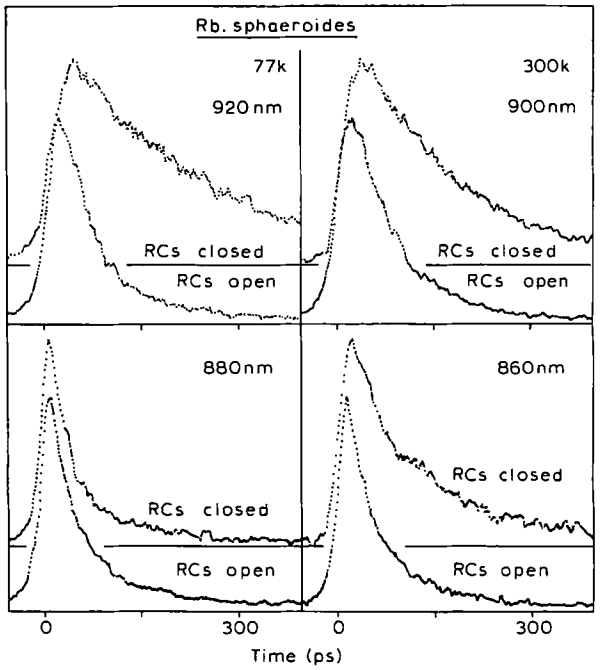

Fig. 6. Fluorescence kinetics of *Rb. sphaeroides* cells as a function of the RCs state, temperature and the recording wavelength. Excitation intensity, 0.3 W/cm^2 at 796 nm, spectral resolution of recording, 4 nm.

Chr. minutissimum [15] is observed both for closed and open RCs when the B800 BChl pool is primarily excited. At selected recording wavelengths the decay is dependent also on the RC state, as shown in Fig. 6 for *Rb. sphaeroides*.

Scheme (2) describes well the main peculiarities of these dependences. By way of example, Figs. 7 and 8 demonstrate a good agreement achieved between the model and experimental kinetic curves for the case of

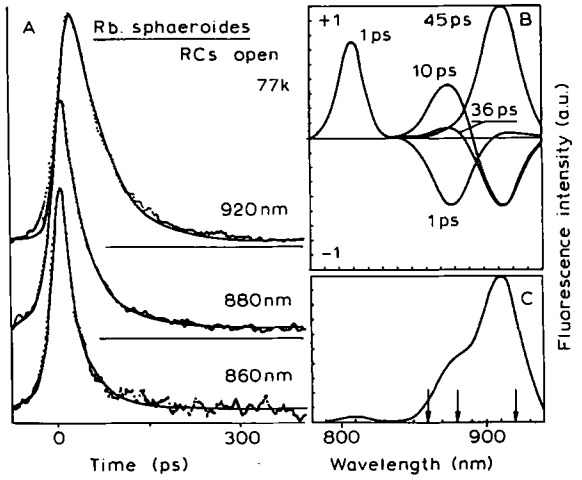

Fig. 7. (A) Experimental fluorescence kinetics (dotted curves) of *Rb. sphaeroides* chromatophores with open RCs at 77 K and simulated model curves (continuous). Excitation and recording conditions as in Fig. 6. Approximation kinetics parameters are the same as in Fig. 4, except that $1/a_{23}(B) = 40$ ps and $1/a_{34} = 45$ ps. (B) and (C) The same as in Fig. 4.

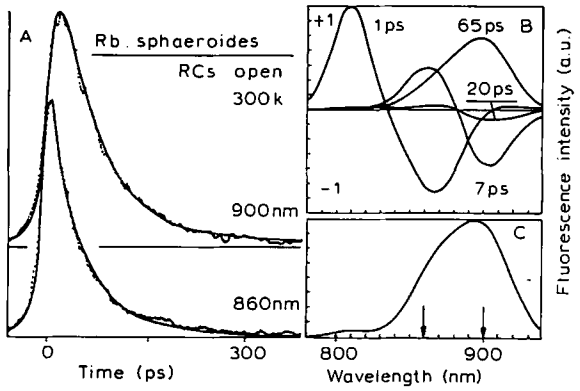

Fig. 8. (A) Experimental fluorescence kinetics (dotted curves) of *Rb. sphaeroides* chromatophores with open RCs at room temperature and simulated model curves (continuous). Kinetic approximation parameters are the same as in the previous figure, except that $1/a_{ii} = 650$ ps. Excitation and recording conditions as in Fig. 6; a flow-cell was used. (B) and (C) The same as in Figs. 4 and 7.

Rb. sphaeroides with open RCs at 77 K and at room temperature. Our previous analysis of the relevant experimental data [14,15] was performed without special model calculations. Therefore, some difficulties with the elucidation of the influence of the RC state on fluorescence kinetics around 860 nm (at room temperature) and around 880–900 nm (at 77 K) were encountered. Now, it is evident that the sensitivity of this kinetics to the RC state is mainly due to the change in the rate constant of the excitation quenching at B875 by (closed or open) RCs. Other rate constants are not sensitive to the RC state. Thus, among the possibilities considered in Refs. 14 and 15, the one suggesting that it is the B875 fluorescence decay that is primarily modulated by the RC state seems to be justified.

It should be stressed, however, that for a reasonably good fitting of theoretical and experimental curves in case of open RCs both at room temperature and at 77 K, the time constant of the B875 excitation trapping should be taken to be about 40–45 ps instead of about 60 ps, as determined numerous times from the low-temperature fluorescence data for *R. rubrum* and *Rb. sphaeroides* [3,4,14]. Otherwise, the B875 fluorescence decay time, calculated at room temperature, corresponding to the overall time of excitation trapping by open RCs in the light-harvesting antenna, would be equal not to 60–70 ps, as has been observed experimentally (see Fig. 8A), but to about 90 ps.

This is another piece of evidence suggesting that model scheme (2) is oversimplified, in the sense that an intrinsic inhomogeneity of the B800, B850 and B875 spectral bands is not taken into account. The effect of this inhomogeneity is that the concentration of excitations on the longest wavelength pigments is higher than expected for spectrally homogeneous bands.

Several publications have appeared lately, in which the experimental evidence suggesting the spectral het-

erogeneity of the B875 absorption band has been presented [13,16,17,24–28]. Although most of the authors of the above-listed papers explain their data by the existence of only two spectral forms within B875, the major B875 and the minor B896, there are a number of arguments to demonstrate that the real situation is much more complicated. Firstly, there is no expected splitting of the long-wavelength absorption band into two distinct bands on cooling down even to 4 K. The spectrum remains relatively broad and unstructured [28]. Secondly, in comparison with a BChl *a* monomer the maximum of the broad fluorescence band of BChl *a* in vivo is remarkably red-shifted (by 15–20 nm) from the maximum of the absorption band. Thirdly, a clear and specific dependence of the fluorescence decay time on the recording wavelength in *R. rubrum* at 77 K has been observed [29,30]. These facts together with the data which have served as the basis for the above-mentioned two-form hypothesis can be explained by assuming that at least the low-temperature spectra are inhomogeneously broadened and there is an effective energy transfer between their homogeneous components [30–32]. The physical reasons for inhomogeneous broadening are various local interactions of different pigments with one another and the surrounding media, which cause shifts in electronic transition energies (for a review, see Ref. 33). The existence of energetically narrow homogeneous spectra within inhomogeneously broadened pigment bands at low temperatures was recently proved by using the hole-burning spectroscopy methods in the case of some artificial pigment-protein complexes [34], native phycobiliproteins (see reviews [35]), and post-etiolated maize leaves [36].

The influence of the exciting light intensity

Most of our measurements have been performed at an average exciting light intensity of the order of 10^{-1} W/cm^2 which, due to the 82 MHz pulse repetition rate, provides the conditions of closed (photooxidized) RCs. An intensity decrease of up to a 100-times has no observable influence on fluorescence kinetics, indicating that neither singlet-singlet nor singlet-triplet excitation annihilation is actual in this intensity range. When the intensity exceeds the value of about 1 W/cm^2 (that corresponds to $5 \cdot 10^{10}$ quanta per cm^2 per pulse), the inclusion of some well-known excitation annihilation effects (see, e.g., review [2]) is clearly displayed for both *Rb. sphaeroides* and *Chr. minutissimum*. These effects include an appreciable shortening of the long-wavelength fluorescence decay time and an evident decline of decay kinetics from exponentiality. For open ($Na_2S_2O_4$-treated) RCs, even at the highest attainable intensities (about $5 \cdot 10^{13}$ quanta per cm^2 per pulse), the changes in fluorescence kinetics have not been reliably detected.

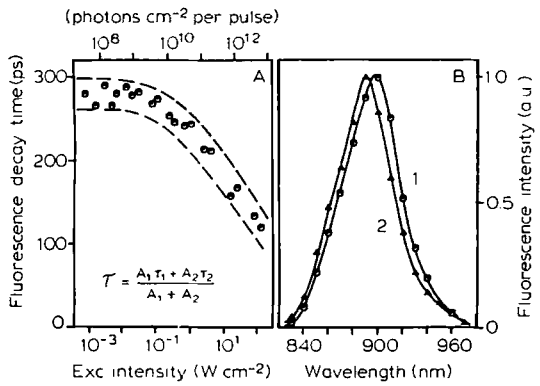

Fig. 9. (A) The dependence of the mean fluorescence decay time (see the text) of *Chr. minutissimum* chromatophores at room temperature on excitation light intensity at 796 nm. Recording at 910 nm with 4 nm bandwidth. There is no forced circulation of suspension in the measuring cell. (B) Room-temperature fluorescence spectra of *Chr. minutissimum* chromatophores for two different excitation light intensities: 1, 0.2 W/cm^2; 2, $1 \cdot 10^3$ W/cm^2.

By way of example, the dependence of the mean decay time of the B875 fluorescence of *Chr. minutissimum* on the exciting light intensity at room temperature and the picosecond fluorescence spectra measured at relatively low and nearly the highest exciting light intensities are shown in Fig. 9. The mean fluorescence decay time was calculated by using the composite amplitudes and lifetimes found by a two-exponential fitting of the measured fluorescence kinetics as follows: $\tau = (A_1 \cdot \tau_1 + A_2 \cdot \tau_2)/(A_1 + A_2)$. Unusually long decay times in these samples at low intensities (about 280 ps, Fig. 9A) are most probably the result of the photoaccumulation of RCs in the state with reduced intermediate acceptor I (state $P1^-Q^-$, where P is the primary electron donor and Q is a quinone acceptor), very much as in the case of *Thiocapsa roseopersicina* [37]. By circulating the chromatophore suspension in the flow-cell the onset of the decline of the fluorescence mean decay time curve as a function of excitation intensity is shifted towards higher intensities (by 1–1.5 orders of magnitude). This shows that under our excitation conditions not the singlet-singlet but the singlet-triplet annihilation processes are dominant.

The blue shift of the fluorescence maximum at high light intensity (Fig. 9B) indicates that in agreement with Monger and Parson [9] the singlet-triplet excitation annihilation proceeds primarily in the B875 antenna complex. This is quite expected, taking into account the perfect energy transfer from B800-850 to B875. As the share of the B850 emission into the whole spectrum in Fig. 9B is relatively small (see, e.g., Fig. 5B, C), the blue shift of the spectrum by some 15% of the whole bandwidth indicates, in full correlation with what was stated above, that the long-wavelength fluorescence band is not homogeneous. This spectral inhomogeneity may favor the localization of excitations in a smaller space

volume of the photosynthetic unit and may in this way enhance the probability of their collision and annihilation.

Most of the experiments by Sundstrom et al. [16] and Van Grondelle et al. [17] have been performed with exciting pulse intensities more than two orders of magnitude higher than those used by us at relatively high pulse repetition rate in the 80 kHz–4 MHz range. Based on the above data, the participation of non-linear excitation processes in some of the picosecond absorption measurements cannot be excluded. In particular, in contrast to the absorption data of Refs. 16 and 17, we have never observed double exponential decay of fluorescence in *R. rubrum* at room temperature, unless high light intensities sufficient to bring about excitation annihilation have been employed or at moderate intensities of the exciting light, when the chromatophores used have not been appropriate quality, containing modified RCs with a damaged primary charge separation chain.

Concluding remarks

This study elucidates the directed nature of the excitation transport taking place in the heterogeneous light-harvesting antenna of purple bacteria. Excitations are transported from the short-wavelength antenna BChl forms to the long-wavelength one, and from the latter to RCs. The same character of excitation transport has been found earlier on cyanobacteria [38], plant cell fragments [39] as well as on green bacteria [40]. According to the electron microscopic data [41], the long-wavelength antenna of purple bacteria is arranged in the form of six pigment-protein globulae, each of which is an immediate neighbour of the RC complex. Thus, the energetically downhill transport of excitations is correlated with their spatial transport towards RCs. This greatly diminishes the overall time of excitation trapping by open RCs as compared with spectrally homogeneous light harvesting antenna of equal size or with a heterogeneous one not having such correlation.

A number of essential kinetic parameters, characterizing the excitation dynamics in the heterogeneous light-harvesting antenna of purple bacteria at 77 K and at room temperature, have been estimated from the comparison of experimental data with the results of model calculations based on the coupled rate equations. In this approach the energy transfer between different pigment pools is described by certain macroscopic kinetic rate constants, and the details of the random walk of the excitations within the pigment pools are neglected:

(i) The intracomplex B800 → B850 transfer time is of the order of 1–2 ps. This conclusion is in close agreement with the suggestion of Refs. 16 and 17.

(ii) The intercomplex B800-B850 → B875 transfer time is less than 10 ps for most (about 70%) excitations. The minor part of the B850 excitations, transferred to B875 complexes in about 50 ps, is likely to belong to the part of B800-850 complexes situated unfavourably (e.g. peripherally) relative to B875. This contradicts the conclusion of Refs. 16 and 17, where a single transfer time of 40–60 ps was distinguished. The presence of two different types of B800-850 complexes, those closely associated with B875-RC complexes and the more remote ones, was recently shown in *Chr. minutissimum* by chemical cross-linkage studies [22]. It seems probable that it is the latter part of B800-850 complexes which is easily detached from the rest of the photosynthetic unit when chromatophores of *Rb. sphaeroides* are fused with liposomes [42].

(iii) The overall excitation trapping time by open RCs is 60–70 ps. This is approximately equal to that in *R. rubrum* [3,4], which has a single type of light-harvesting complexes, B875. Thus, purple bacteria, having photosynthetic units of considerably different sizes, are characterized by close values of overall trapping times and, consequently, of the quantum yields of the primary charge separation.

Unfortunately, this simple and transparent model has some drawbacks as was already noted before. We are of the opinion that this is due to the fact that the inner heterogeneity of the pigment pools has not been taken into account. It is possible that the necessity for the inclusion of at least two B800-850 complexes in our model is also a reflection of this heterogeneity. On the other hand, there are macroscopic structural data supporting the two-type hypotheses of the B800-850 complexes [21,22].

It is worth noting that the assignment of two lifetimes (e.g. 10–20 ps and 150–200 ps according to Ref. 29) to the B875 excited state decay (which is like to the model used in Refs. 16 and 17) does not lead to the more simple model. For a satisfactory fit of the experiment it is still necessary to take into account some extra B800-850 complexes. The possibility of including all the essential heterogeneities of the system (not only of B875) into the kinetic model calculations is now under study in this laboratory.

The two picosecond spectroscopic approaches based on the detection of transient absorption and fluorescence spectra give, in principle, mutually complementary information about excitation dynamics in the heterogeneous light-harvesting antenna of purple bacteria. Obviously, both methods should lead to the same basic conclusions on the matter and the kinetic parameters, provided the results of the measurements are appropriately treated. At the present stage of investigation, there is only a general agreement between the interpretation of picosecond absorption [16,17] and picosecond fluorescence (Refs. 14, 15, this work) data. For example, when our experimental decay curves are fitted in the framework of scheme (1), i.e. without

taking into consideration the existence of the two types of B800-850 complexes (see Figs. 2, 3 and the data in Ref. 14), the calculated parameters, in particular, for B850 → B875 transfer are about the same as those found in Refs. 16 and 17. A comprehensive understanding of the noted discrepancies needs a detailed analysis of the corresponding experimental situation and adequate model calculations.

Appendix

The following basic model scheme has been used to describe the excitation transfer between distinct antenna pigment pools and RCs:

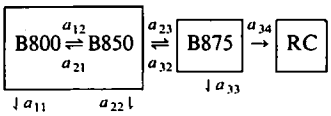

(A1)

The time dependence of the excited state concentration $n_i(t)$ for each antenna pool, B800, B850, B875, can be found under low-intensity excitation conditions from a system of three coupled kinetic rate equations:

$$dn_i(t)/dt = \sum_{j=1}^{3} [a_{ji} n_j(t) - a_{ij} n_i(t)] - n_i(t) a_{ii} - \delta_{3i} n_i(t) a_{34} \quad (A2)$$

($i = 1; 2; 3$)

In the case of δ-pulse excitation, the decay kinetics in each pool is expressed by

$$n_i(t) = \sum_{j=1}^{3} c_{ij} \exp(-t/\tau_j) \quad (A3)$$

($i = 1; 2; 3$), where the amplitudes c_{ij} are determined by the initial concentrations of the excited states at each pool and by the rate constants a_{ij}.

The dependence of fluorescence kinetics on the recording wavelength has been described by the following equation:

$$I(\lambda, t) = \sum_{i=1}^{3} F_i(\lambda) n_i(t) \quad (A4)$$

where $F_i(\lambda)$ is the fluorescence spectrum of the ith pigment pool, taken from the experiment. For a comparison with experimental kinetics all the theoretical curves $I(\lambda, t)$ should be convoluted with the apparatus response function.

To obtain the stationary fluorescence spectra the time integration of equation (A4) has been performed:

$$I(\lambda) = \int_0^\infty I(\lambda, t)\, dt = \sum_{i=1}^{3} F_i(\lambda) \sum_{j=1}^{3} c_{ij} \tau_j \quad (A5)$$

The spectral distribution of the amplitude of the jth kinetic component, characterized by the lifetime τ_j, has been revealed from the equation

$$A_j(\lambda) = \sum_{i=1}^{3} c_{ij} F_i(\lambda) \quad (A6)$$

All the rate constants for uphill excitation transfer were calculated by using the Forster approximation for the pairwise rates of excitation transfer [43] as follows:

$$a_{ji} = a_{ij} \frac{z_i \int \epsilon_i(\nu) F_j(\nu) \frac{d\nu}{\nu^4}}{z_j \int \epsilon_j(\nu) F_i(\nu) \frac{d\nu}{\nu^4}} \quad (A7)$$

Here z_i, z_j are the numbers of BChl molecules of the ith and jth pigment pools, $F_i(\nu)$ is the corresponding normalized fluorescence spectrum, so that $\int F_i(\nu) d\nu = 1$, and $\epsilon_i(\nu)$ is the absorption coefficient in 1/cm. The downhill rate constants a_{ij} were supposed to be the parameters of the model. For calculations the experimental fluorescence and absorption spectra from Refs. 11, 19, 20, 28 and 44, measured at room temperature and at 77 K, have been used together with the results of our own measurements. To simplify computations the band-shapes of the spectra were approximated with the Gaussians of the preserved widths and band maxima.

Acknowledgements

We thank Professor A. Yu. Borisov and Professor K. Rebane for reading the manuscript and for the valuable remarks, Dr. W. Sundstrom for helpful discussions, Dr. S.G. Kharchenko and I.V. Bukhova for the preparation of chromatophores.

References

1 Borisov, A.Yu. and Godik, V.I. (1973) Biochim. Biophys. Acta 301, 227–248.
2 Van Grondelle, R. (1985) Biochim. Biophys. Acta 811, 147–195.
3 Freiberg, A., Godik, V.I. and Timpmann, K. (1984) in Advances in Photosynthesis Research (Sybesma, C., ed.), Vol. 1, pp. 45–48, Martinus Nijhoff/Dr. W. Junk, Dordrecht, The Netherlands.
4 Borisov, A.Yu., Freiberg, A.M., Godik, V.I., Rebane, K.K. and Timpmann, K.E. (1985) Biochim. Biophys. Acta 807, 227–229.
5 Borisov, A.Yu. and Fetisova, Z.G. (1971) Mol. Biol. 5, 509–517.
6 Seely, G.R. (1973) Theor. Biol. 40, 173–199.
7 Fetisova, Z.G., Borisov, A.Yu. and Fok, M.V. (1984) Theor. Biol. 112, 41–75.
8 Drews, G. (1985) Microbiol. Rev. 49, 59–70.
9 Monger, T.G. and Parson, W.W. (1977) Biochim. Biophys. Acta 460, 393–407.
10 Zankel, K.L. and Clayton, R.K. (1969) Photochem. Photobiol. 9, 7–15.
11 Meinhardt, S.W., Kiley, P.J., Kaplan, S., Crofts, A.R. and Harayama, S. (1985) Arch. Biochem. Biophys. 236, 130–139.
12 Jackson, W.J., Prince, R.C., Stewart, G.J. and Marrs, B.L. (1986) Biochemistry 25, 8440–8446.

13 Sebban, P. and Moya, I. (1983) Biochim. Biophys. Acta 722, 436–442.
14 Godik, V.I., Timpmann, K.E., Freiberg, A.M., Borisov, A.Yu. and Rebane, K.K. (1986) Dokl. Akad. Nauk. SSSR 289, 714–718.
15 Godik, V.I., Freiberg, A.M., Timpmann, K.E., Borisov, A.Yu. and Rebane, K.K. (1987) in Progress in Photosynthesis Research (Biggins, I., ed.), Vol. 1, pp. 41–44, Martinus Nijhoff Publishers, Dordrecht, The Netherlands.
16 Sundstrom, V., Van Grondelle, R., Bergstrom, H., Akesson, E. and Gillbro, T. (1986) Biochim. Biophys. Acta 851, 431–446.
17 Van Grondelle, R., Bergstrom, H., Sundstrom, V. and Gillbro, T. (1987) Biochim. Biophys. Acta 894, 313–326.
18 Freiberg, A. (1986) Laser Chem. 6, 233–252.
19 Van Grondelle, R., Kramer, H.J.M. and Rijgersberg, C.R. (1982) Biochim. Biophys. Acta 682, 208–215.
20 Sebban, P., Jolchine, G. and Moya, I. (1984) Photochem. Photobiol. 39, 247–253.
21 Peters, I., Takemoto, J. and Drews, G. (1983) Biochemistry 22, 5660–5667.
22 Moskalenko, A.A. and Toropygina (1987) Dokl. Akad. Nauk SSSR 296, 483–486.
23 Visser, A.J.W.G., ed. (1985) Time-Resolved Fluorescence Spectroscopy a special issue of Analytical Instrumentation, Vol. 14, 3&4.
24 Bolt, J.D., Hunter, C.N., Niederman, R.A. and Sauer, K. (1981) Photochem. Photobiol. 34, 653–656.
25 Gomez, I., Del Campo, F.F. and Ramirez, J.M. (1982) FEBS Lett. 141, 185–188.
26 Borisov, A.Yu., Gadonas, R.A., Danielius, R.V., Piskarskas, A.S. and Razjivin, A.P. (1982) FEBS Lett. 138, 25–28.
27 Kramer, H.J.M., Pennoyer, J.D., Van Grondelle, R., Westerhuis, W.H.J., Niederman, R.A. and Amesz, J. (1984) Biochim. Biophys. Acta 767, 335–344.
28 Van Dorssen, R.J. (1988) Thesis, Leiden University.
29 Freiberg, A., Godik, V.I. and Timpmann, K. (1987) in Progress in Photosynthesis Research (Biggins, J., ed.), Vol. 1, pp. 45–48, Martinus Nijhoff Publishers, Dordrecht, The Netherlands.
30 Godik, V.I., Freiberg, A.M. and Timpmann, K.E. (1988) Dokl. Akad. Nauk SSSR 298, 1469–1473.
31 Gulis, I.M. and Komiak, A.I. (1977) Zh. prikl. spektr. 27, 841–845.
32 Avarmaa, R., Jaanisoo, R., Mauring, K., Renge, I. and Tamkivi, R. (1986) Mol. Phys. 57, 605–621.
33 Avarmaa, R.A. and Rebane, K.K. (1985) Spectrochim. Acta 41A, 1365–1380.
34 Boxer, S.G., Gottfried, D.S., Lockhart, D.J. and Middendorf, T.R. (1987) J. Chem. Phys. 86, 2439–2441.
35 Friedrich, J. and Haarer, D. (1984) Angew. Chem. (Int. Ed.) 23, 113–140.
36 Mauring, K., Renge, I. and Avarmaa, R. (1987) FEBS Lett. 223, 165–168.
37 Godik, V.I., Timpmann, K.E., Freiberg, A.M., Borisov, A.Yu. and Rebane, K.K. (1985) Dokl. Akad. Nauk. SSSR 284, 491–494.
38 Porter, G., Tredwell, C.J., Searle, G.F.W. and Barber, J. (1978) Biochim. Biophys. Acta 501, 232–245.
39 Avarmaa, R.A., Kochubey, S.M. and Tamkivi, R.P. (1979) FEBS Lett. 102, 139–142.
40 Freiberg, A.M., Timpmann, K.E. and Fetisova, Z.G. (1988) in Green Photosynthetic Bacteria (Olson, J.M., ed.), pp. 81–90, Plenum, New York, NY, U.S.A.
41 Miller, K.R. (1982) Nature 300, 53–55.
42 Pennoyer, J.D., Kramer, H.J.M., Van Grondelle, R., Westerhuis, W.H.J., Amesz, J. and Niederman, R.A. (1985) FEBS Lett. 182, 145–150.
43 Agranovich, V.M. and Galanin, M.D. (1982) Electronic Excitation Energy Transfer in Condensed Matter, North-Holland, Amsterdam.
44 Rijgersberg, C.P., Van Grondelle, R. and Amesz, J. (1980) Biochim. Biophys. Acta 592, 53–64.
45 Prokhorenko, I.R., Serdiuk, O.P., Toropygina, O.A. and Erokhin, Yu.E. (1981) Dokl. Akad. Nauk SSSR 256, 496–499.